Simultaneous generation of controllable double white light lasers by focusing an intense femtosecond laser pulse in air

Yaoxiang Liu (刘尧香)[1,2,3], Tie-Jun Wang (王铁军)[2,3,*], Na Chen (陈 娜)[2,3], Hao Guo (郭 豪)[2,3], Haiyi Sun (孙海轶)[2,3], Lu Zhang (张 璐)[4], Zheng Qi (齐 征)[4], Yuxin Leng (冷雨欣)[2,3], Zhanshan Wang (王占山)[1], and Ruxin Li (李儒新)[2,3]

[1]*MOE Key Laboratory of Advanced Micro-structured Materials, Institute of Precision Optical Engineering, School of Physics Science and Engineering, Tongji University, Shanghai 200092, China*

[2]*State Key Laboratory of High Field Laser Physics and CAS Center for Excellence in Ultra-intense Laser Science, Shanghai Institute of Optics and Fine Mechanics, Chinese Academy of Sciences, Shanghai 201800, China*

[3]*Center of Materials Science and Optoelectronics Engineering, University of Chinese Academy of Sciences, Beijing 100049, China*

[4]*Science and Technology on Space Physics Laboratory, Beijing 100076, China*

**Corresponding author: tiejunwang@siom.ac.cn*

Received July 20, 2020; accepted August 28, 2020; posted online October 14, 2020

We report on a simultaneous generation of double white light lasers through filamentation by focusing a femtosecond laser pulse. The appearance of the two white light lasers can be controlled by tilting the focusing lens. The spectral bandwidth and the pulse energy of the double white light lasers were controlled by tuning laser filamenting pulse energy and polarization. Two white light lasers with pulse energies of 1.54 mJ and 1.84 mJ, respectively, were generated with the pump laser energy of 7.43 mJ. Besides being beneficial in understanding the multiple white light lasers generation process through multiple filamentation and its control, the results are also valuable for white light laser-based applications.

Keywords: filamentation; white light laser; polarization.

doi: 10.3788/COL202018.121402.

Propagation of an ultrashort intense pulse laser beam in transparent media is one of the research frontiers in nonlinear optics due to the complex physics of nonlinear effects and its wide range of applications[1–4]. One of the remarkable applications is the generation of supercontinuum (SC) from filamentation, which was firstly, to the best of our knowledge, investigated in 1986[5]. The spectrum of Ti:sapphire laser-based white light or SC spans from the ultraviolet to the infrared wavelength. Moreover, the white light produced by the ultrashort intense laser pulse through filamentation has been proved to be spatially and temporally coherent[6,7], which is more critical to SC for ultrafast spectroscopy applications to achieve higher accuracy, efficiency, and speed with lower cost. The filament-based coherent white light laser source finds extensive applications in biomedical imaging[8], molecular fingerprint spectroscopy[9], optical coherence tomography[10], tunable ultrafast pulse generation[11], few-cycle femtosecond pulses compression[12], LIDAR for atmospheric remote sensing[13–15], etc. Kerr and plasma-nonlinearities-based self-phase modulation (SPM), self-steepening, and four wave mixing are the basic mechanisms proposed for broadband SC generation[16,17]. The evolutions of SC generation through filamentation have been investigated under the conditions of free propagation, loose and tight focusing[18–21], and different initial laser polarizations[19,22].

The tilting lens has been used to control filament properties such as the number, cross pattern, and structure through introducing aberration by focusing femtosecond laser pulses[23–26]. Meanwhile, formation of SCs was also studied[25,27,28]. Compared with these works, in our work, we make use of the well investigated astigmatism control technique simply by tilting the focal lens to control the appearance of the double white light lasers. The appearance of the two white light lasers is related to the tilting-lens-controlled filaments. The most important is that these two white light lasers can be controlled by pump laser polarization. Spectral and energy measurements of each white light laser were performed separately when changing the laser polarization. Our results reveal that the two white light lasers can be controlled by manipulating the laser intensity inside the filaments through pump laser energy and polarization.

A laser pulse generated from a Ti:sapphire laser pulse amplifier was focused by an $f = 50$ cm lens to create filaments in air [Fig. 1(a)]. The beam diameter is of 12 mm with a central wavelength at 800 nm, repetition rate of 1 kHz, and pulse duration of 32 fs. A zero-order quarter waveplate (QWP) was used to tune the polarization of the laser pulse for filamentation. Laser polarization changed from linear polarization (LP) to circle polarization (CP) when the QWP angle was rotated from 0 deg

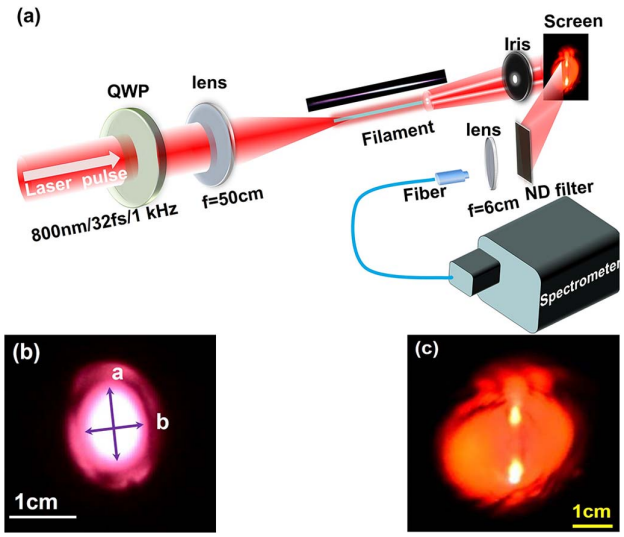

Fig. 1. (a) Schematic of experimental setup. QWP is a zero-order quarter waveplate. ND filter is neutral density filter. (b) Input beam spatial profile and (c) typical forward beam pattern after filamentation (about 1.3 m away) on the screen taken by a digital camera (Nikon D7200). The laser pulse energy was 7.43 mJ.

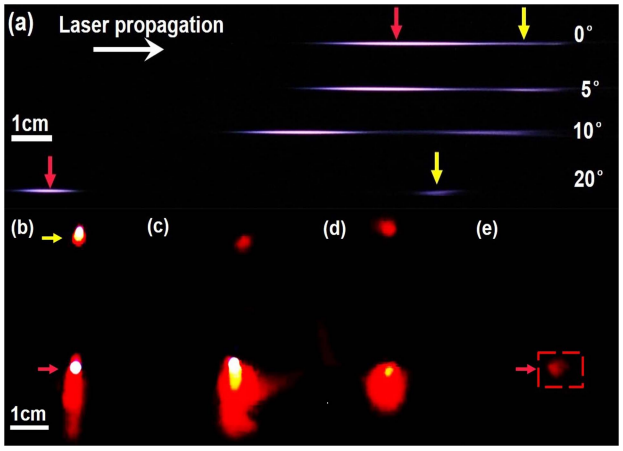

Fig. 2. (a) Real-color images of filaments in air with laser incident angle to the lens changing from 0 deg to 20 deg. Exposure time of the camera in (a) was 0.25 s. The energy of the linearly polarized laser pulse was 7.43 mJ. Corresponding forward white light beam patterns on the screen at different incident angles of (b) 0 deg, (c) 5 deg, (d) 10 deg, and (e) 20 deg. Exposure time of the camera in (b)–(e) was 0.02 s with an ND filter in front of the camera. There are 20 shots of white light beams accumulated in each image.

to 45 deg. An iris with a diameter of 3 mm was placed on the beam path after filamentation to select and let only one white light laser pass through for spectrum and energy analysis. The forward white light lasers were scattered by a white diffusion plate and collected by a 2 in. (1 in. = 2.54 cm) focusing lens ($f = 6$ cm) to a fiber coupled to a CCD-based spectrometer (Princeton Instruments, SP-2560. 150 g/mm, blaze wavelength at 500 nm) for spectral analysis. The exposure time of the CCD was 100 ms, and the spectral signals obtained by the spectrometer were averaged five times. A neutral density (ND) filter was inserted before the collecting lens to attenuate the diffused laser intensity. The initial beam profile is shown in Fig. 1(b), which is slightly elliptical ($a/b = 1.3$, $a = 1.45$ cm, $b = 1.17$ cm) with a diffraction ring structure. By focusing the initial pump laser with energy of 7.43 mJ, the typical forward beam pattern after filamentation (about 1.3 m away) on the screen is shown in Fig. 1(c) taken by a digital camera (Nikon D7200) with an inclination angle of 10 deg from the laser propagation. The peak power of the pump laser pulse was approximately 230 GW ($71P_{cr}$), which is many times the critical power P_{cr}[16] for self-focusing. Multiple filamentation (MF) induced by focusing the high peak power filamenting pulse having an elliptical beam profile with diffraction rings is responsible for the generation of double white light lasers in air[26,29].

Figure 2(a) shows the real-color images of filaments induced by a femtosecond laser with the energy of 7.43 mJ in air. When the incident angle of the laser to the lens was 0 deg, two bright white light spots were generated, as shown in Fig. 2(b). This is caused by input beam astigmatism due to the asymmetrical structure of the pump laser beam pattern, which is elliptical and with diffraction rings[26,29]. The incident angle was changed by rotating the focus lens clockwise in the horizontal plane. As the incident angle of the laser increased gradually by tilting the focusing lens more[24–28], the filament developed into two distinct parts along the propagation path, as indicated by the red and yellow arrows in Fig. 2(a). Simultaneously, the filament location moved towards to the focal lens. The astigmatism of the input laser beam was modified by tilting the focal lens. SC dynamics has been studied when changing the angle of the focal lens[25,27,28]. Large astigmatism can change the distribution of the filaments, determine the filament number, and induce filament spatial splitting[23–28]. The second part of the filament indicated by the yellow arrow became short and nearly invisible when the incident angle of the laser turned to 20 deg. Simultaneously, both of the forward white light shots on the screen were weaker, and the upper one that is indicated by the red arrow [Fig. 2(b)] faded away [Fig. 2(e)] with the second part of the filament getting weaker. Then, it is reasonable to confirm that the upper white light is produced by the second part of the filament, and the lower one is produced by the first part of the filament.

Figure 3(a) shows the real-color fluorescence images of filaments when the laser polarization changes from LP to CP by rotating the QWP angle from 0 deg to 45 deg . The laser pulse energy was 7.43 mJ. The filament length decreases as the laser polarization changes from LP to CP[30]. With high pump laser energy, the filament becomes longer. The pixel intensity in the yellow rectangle, as shown Fig. 3(a), was integrated to obtain the fluorescence intensity distribution along the filament. The full width of the fluorescence intensity curve at 3σ is defined as the effective length of the filament. Here, σ is the standard

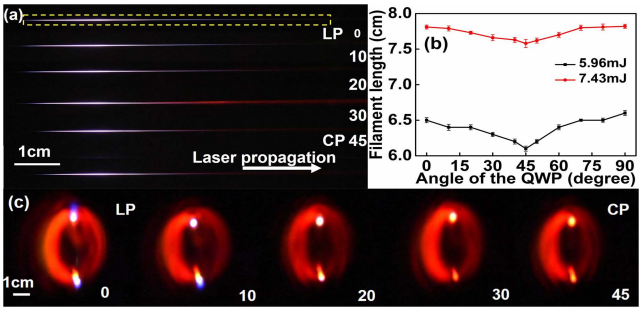

Fig. 3. (a) Filament fluorescence images under different polarization states taken by a camera with the exposure time of 0.25 s. The laser energy was 7.43 mJ. The laser polarization is LP (CP) when the QWP angle was 0 deg or 90 deg (45 deg). (b) The effective filament length as a function of the QWP angle (the laser polarization state) under different laser energies. (c) The corresponding forward white light spots in (a) as the polarization states of the laser changed from LP to CP. The exposure time of the camera in (c) was 0.02 s without the ND filter.

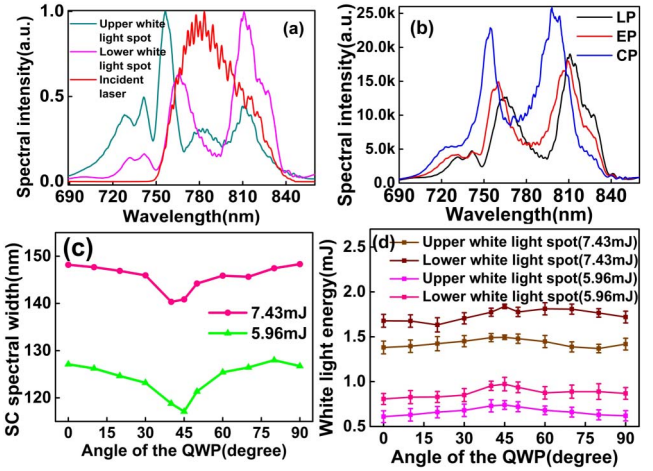

Fig. 4. (a) Normalized SC spectra of the upper and lower white light spots for LP filamenting pulses. The pulse energy was 7.43 mJ. (b) Spectra of white lights for LP, EP (the QWP angle was 30 deg), and CP. The spectral intensity is the integration of the spectral density of both the upper and lower white lights. (c) Spectral bandwidth of the SC versus different pump laser polarization states. The spectral bandwidth is defined by the full width of the spectral intensity curve at 3σ. σ is the standard deviation of the spectral noise. (d) Energy of each white light as a function of the pump laser polarization state under different pump laser energies.

deviation of the noise. Figure 3(b) gives the effective filament length under different laser polarization states quantitatively when the laser energy is 5.96 mJ and 7.43 mJ, respectively. The corresponding forward white light shots for pulse energy of 7.43 mJ are shown in Fig. 3(c) under different polarizations. The white light brightness dims as the polarization states of the laser changed from LP to CP.

The normalized SC spectra of the upper and lower white light spots are shown in Fig. 4(a) for LP filamenting pulses. Each spectral distribution intensity was normalized at its maximum. The laser energy was 7.43 mJ. Compared with the initial spectra of the incident laser before the filament, the spectra of the upper and lower white light spots are both broadened. The spectrum of the upper white light differs slightly from that of the lower one. For the upper one, the spectral intensity in the shorter wavelength range (690–770 nm) is stronger than that in the longer wavelength range (800–840 nm), while it is the opposite for the lower white light. The SC spectra of white lights for LP, elliptical polarization (EP, the QWP angle is 30 deg), and CP are shown in Fig. 3(b). The spectral intensity curves are obtained by integrating the spectral intensities of both the upper and lower white lights. As the laser polarization changes from LP to CP, the SC spectral intensity increases. The spectral bandwidth of white light lasers decreases simultaneously, as shown in Fig. 3(c). The spectral bandwidth is defined by the full width of the spectral intensity curve at 3σ. σ is the standard deviation of the spectral noise. The SC spectral bandwidth becomes broader with higher laser pulse energy. The polarization dependent measurement of two white light pulse energies shows that CP favors stronger white light generation as compared with the LP filamenting pulse [Fig. 4(d)]. When measuring pulse energy of each white light beam, an iris with a diameter of 3 mm was placed in the light path to let only one white light beam pass through. A similar polarization effect was observed for single white light generation through filamentation[31]. Under the circularly polarized pump energy of 7.43 mJ for filamentation in air, two white light lasers with pulse energies of 1.54 mJ and 1.84 mJ, respectively, were generated. These pulses are intense enough for applications of ultrafast laser spectroscopy[8–12].

The electronic mechanism of SPM is the fundamental physics of SC generation. For a pump laser with the electromagnetic wave of $E(t) = E_0 e^{\frac{-t^2}{T^2}} \cos[\omega_0 t - \frac{n(t)\omega_0 z}{c}]$ propagating in a nonlinear medium, the refractive index modulated by the pump laser intensity Δn and frequency change $\Delta\omega$ can be expressed as[32] $\Delta n = n_2 E_0^2 e^{-t^2/T^2} \cos(\omega_0 t)$ and $\Delta\omega = (-\frac{\omega_0}{n_0 c}) L \Delta n$, respectively, where $n_2 = 3\chi^{(3)}/4c\varepsilon_0 n_{02}$ is the nonlinear refractive index, $\chi^{(3)}$ is the third-order nonlinearity, and L is the effective interaction length of the pump laser in the medium. The third-order nonlinearity $\chi^{(3)}$ decreases when the polarization state of the pump laser changes from LP to CP[33]. Then, at the leading $(\partial I/\partial t > 0)$ and trailing $(\partial I/\partial t < 0)$ edges of the laser pulse, more blue-shift and red-shift frequencies are produced for the LP pump laser as compared to the CP pump laser. Besides, due to the SPM caused by plasma, the frequency change is $\Delta\omega = -\frac{2\pi e^2}{c m_e \omega_0} l \frac{\partial[N_e(t)]}{\partial t}$ [16], where e is the electron charge, m_e is the electron mass, $N_e(t)$ is the electron density, and l is the effective interaction length of the pump pulse in the plasma. Because $l = ct$, then $\Delta\omega \propto \partial[N_e(z)]/\partial z$. Each 'slice' of the laser pulse at the trailing edge would

encounter a plasma increase, that is $\partial[N_e(z)]/\partial z > 0$, which contributes to the blue shift of the wavelength. Due to the longer plasma channel [Fig. 3(b)] and higher plasma density being generated by LP rather than the CP pump laser pulse[31] or with high pulse energy [Fig. 3(b)], then, a white light laser with broader bandwidth is generated through filamentation by using the LP laser pulse [Fig. 4(c)] or higher pulse energy [Fig. 4(c)]. Since the two white lights are generated by different parts of filaments, the spectrum of each white light can be manipulated by controlling laser intensity inside the filament [Fig. 4(a)]. Because the clamping intensity in an air filament is higher for CP laser pulse than that for LP laser pulse[34,35], the white light intensity, which is directly related with pump laser intensity, is thus higher for the CP pump pulse [Figs. 4(b) and 4(d)].

In summary, we demonstrate the simultaneous generation of double white light lasers from a femtosecond laser filament in air. The control of the appearance of the two white lights was achieved by tilting the focusing lens. The corresponding relationship between the two filaments and the two white light lasers was confirmed. The spectrum and pulse energy of each white light were manipulated by controlling the filamenting pulse polarization. Using the LP pump laser, a longer filament and wider spectral range of white light were obtained compared with that of the CP pump laser, whereas, the CP pump laser pulse increased the pulse energies of two white lights. Two white light lasers with pulse energies of 1.54 mJ and 1.84 mJ, respectively, were generated in air with the CP pump energy of 7.43 mJ for filamentation. We believe that in addition to being beneficial in understanding the white light generation process through MF and its control, the results of this study can also provide a novel and more convenient method to provide controllable multiple white light laser sources, which is significantly valuable for white light laser-based applications.

This work was supported in part by the Strategic Priority Research Program of the Chinese Academy of Sciences (No. XDB16010400) and the International Partnership Program of Chinese Academy of Sciences (No. 181231KYSB20160045). The authors thank Prof. See Leang Chin from Laval University in Canada for the fruitful discussions.

References

1. X. M. Zhao, J. C. Diels, C. Y. Wang, and M. Elizondo, IEEE J. Quantum Electron. **31**, 599 (1995).
2. B. La Fontaine, F. Vidal, Z. Jiang, C. Y. Chien, D. Comtois, A. Desparois, T. W. Johnson, J.-C. Kieffer, H. Pépin, and H. P. Mercure, Phys. Plasma **6**, 1615 (1999).
3. O. G. Kosareva, V. P. Kandidov, A. Brodeur, C. Y. Chien, and S. L. Chin, Opt. Lett. **22**, 1332 (1997).
4. E. T. J. Nibbering, P. E. Curley, G. Grillon, B. S. Prade, M. A. Franco, F. Salin, and A. Mysyrowicz, Opt. Lett. **21**, 62 (1996).
5. P. B. Corkum, Rolland Claude, and T. Srinivasanrao, Phys. Rev. Lett. **57**, 2268 (1986).
6. A. K. Dharmadhikari, F. A. Rajgara, N. C. S. Reddy, A. S. Sandhu, and D. Mathur, Opt. Express **12**, 695 (2004).
7. P. A. Zhokhov, A. A. Voronin, I. V. Fedotov, A. B. Fetotov, and A. M. Zheltikov, Phys. Rev. A **87**, 013819 (2013).
8. H. H. Tu and A. Boppart, Laser Photon. Rev. **7**, 628 (2013).
9. C. R. Petersen, U. Møller, I. Kubat, B. Zhou, S. Dupont, J. Ramsay, T. Benson, S. Sujecki, N. Abdel-Moneim, Z. Tang, D. Furniss, A. Seddon, and O. Bang, Nat. Photon. **8**, 830 (2014).
10. G. Humbert, W. Wadsworth, S. Leon-Saval, J. Knight, T. Birks, P. S. J. Russell, M. Lederer, D. Kopf, K. Wiesauer, E. Breuer, and D. Stifter, Opt. Express **14**, 1596 (2006).
11. F. Theberge, N. Akozbek, W. Liu, A. Becker, and S. L. Chin, Phys. Rev. Lett. **97**, 023904 (2006).
12. P. Prem Kiran, S. Bagchi, C. L. Arnold, S. Sivaram Krishnan, G. Ravindra Kumar, and A. Couairon, Opt. Express **18**, 21504 (2010).
13. J. Kasparian, M. Rodriguez, G. Méjean, J. Yu, E. Salmon, H. Wille, R. Bourayou, S. Frey, Y.-B. André, A. Mysyrowicz, R. Sauerbrey, J.-P. Wolf, and L. Wöste, Science **301**, 61 (2003).
14. L. Wöste, C. Wedekind, H. Wille, P. Rairoux, B. Stein, S. Nikolov, C. Werner, S. Niedermeier, F. Ronneberger, H. Schillinger, and R. Sauerbrey, Las. Optoelektron **29**, 51 (1997).
15. R. Rairoux, H. Schillinger, S. Niedermeier, M. Rodriguez, F. Ronneberger, R. Sauerbrey, B. Stein, D. Waite, C. Wedekind, H. Wille, L. Wöste, and C. Ziener, Appl. Phys. B **71**, 573 (2000).
16. A. Couairona and A. Mysyrowicz, Phys. Rep. **441**, 47 (2007).
17. L. Bergé, S Skupin, R. Nuter, J. Kasparian, and J.-P. Wolf, Rep. Prog. Phys. **70**, 1633 (2007).
18. J. Kasparian, R. Sauerbrey, D. Mondelain, S. Niedermeier, J. Yu, J.-P. Wolf, Y.-B. André, M. Franco, B. Prade, S. Tzortzakis, A. Mysyrowicz, M. Rodriguez, H. Wille, and L. Wöste, Opt. Lett. **25**, 1397 (2000).
19. H. Yang, J. Zhang, Q. Zhang, Z. Hao, Y. Li, Z. Zheng, Z. Wang, Q. Dong, X. Lu, Z. Wei, Z. Sheng, J. Yu, and W. Yu, Opt. Lett. **30**, 534 (2005).
20. W. Liu, S. Petita, A. Becker, N. Aközbekb, M. Bowden, and S. L. Chin, Opt. Commun. **202**, 189 (2002).
21. P. Prem Kiran, S. Bagchi, S. R. Krishnan, C. L. Arnold, G. Ravindra Kumar, and A. Couairon, Proc. SPIE **7728**, 77281P (2010).
22. M. Kolesik, J. V. Moloney, and E. M. Wright, Phys. Rev. E **64**, 046607 (2001).
23. Y. Fu, H. Gao, W. Chu, J. Ni, H. Xiong, H. Xu, J. Yao, B. Zeng, W. Liu, Y. Cheng, Z. Xu, and S. L. Chin, Appl. Phys. B **103**, 435 (2011).
24. A. A. Dergachev, A. A. Ionin, V. P. Kandidov, D. V. Mokrousova, L. V. Seleznev, D. V. Sinitsyn, E. S. Sunchugasheva, S. A. Shlenov, and A. P. Shustikova, Quantum Electron. **44**, 1085 (2014).
25. N. G. Ivanov, V. F. Losev, V. E. Prokop'ev, and K. A. Sitnik, Opt. Commun. **387**, 322 (2017).
26. G. Fibich, S. Eisenmann, B. Ilan, and A. Zigler, Opt. Lett. **29**, 1172 (2004).
27. Y. Kamali, Q. Sun, J.-F. Daigle, A. Azarm, J. Bernhardt, and S. L. Chin, Opt. Commun. **282**, 950 (2009).
28. S. Sreeja, T. S. Prashant, C. Leela, V. R. Kumar, S. P. Tewari, S. V. Rao, and P. P. Kiran, Proc. SPIE **8434**, 84340T (2012).
29. A. Dubietis, G. Tamošauskas, G. Fibich, and B. Ilan, Opt. Lett. **29**, 1126 (2004).
30. Z. B. Zhu, T. J. Wang, Y. X. Liu, N. Chen, H. Zhang, H. Y. Sun, H. Guo, J. H. Zhang, X. Zhang, G. Li, C. P. Liu, Z. N. Zeng, J. S. Liu, S. L. Chin, R. X. Li, and Z. Z. Xu, Chin. Opt. Lett. **16**, 073201 (2018).

31. N. Chen, T. J. Wang, Z. B. Zhu, H. Guo, Y. X. Liu, F. K. Yin, H. Y. Sun, Y. X. Leng, and R. X. Li, Opt. Lett. **45**, 4444 (2020).
32. Y. Q. Liu, J. Zhang, Z. Jin, Z.Q. Hao, Z. Zhang, and Z. H. Wang, Appl. Phys. B **92**, 153 (2008)
33. S. Petit, A. Talebpour, A. Proulx, and S. L. Chin, Opt. Commun. **175**, 323 (2000).
34. X. Zhang, T. J. Wang, H. Guo, N. Chen, L. Lin, L. G. Zhang, H. Y. Sun, J. Liu, J. S. Liu, B. F. Shen, R. X. Li, and Z. Z. Xu, arXiv:1902.03432v1 (2019).
35. N. A. Panov, V. A. Makarov, V. Y. Fedorov, and O. G. Kosareva, Opt. Lett. **38**, 537 (2013).